The thermo-optical coupling in optical resonators

S.V. Dhurandhar[1], P. Hello[2], B.S. Sathyaprakash[1] and J-Y. Vinet[2]

[1] *Inter-University Centre for Astronomy and Astrophysics, Post Bag 4, Ganeshkhind, Pune 411007, INDIA*

[2] *Groupe Virgo, Laboratoire de l'Accelerateur Lineaire, Universite de Paris-Sud, Batiment 208, 91405 Orsay, France*

Abstract

Interferometric detectors of gravitational waves employ long baseline Fabry-Perot cavities with stored power of the order of 10 kW. The mirrors have a high reflectivity with absorption coefficient of a few parts in a million. The laser beam therefore acts as a source of heat creating a thermal gradient in the substrate and the consequent deformation in the mirror which in turn modifies the intra-cavity light field. The problem is thus coupled and non-linear. Though the effect is expected to be negligible in the case of initial interferometers future interferometers are expected to employ much higher powers and it is necessary to ascertain thermo-elastic deformations and their effect on the stability of the laser field in the cavity. In this paper, which is first in a series to study instabilities in giant high power laser cavities, we have analytically solved the coupled problem of thermo-elastic deformations and their effect on the laser field, perturbatively and we show that within the realm of our (physically reasonable) assumptions there are no instabilities in the frequency range of 1 Hz–1 kHz.

I. INTRODUCTION

Gravitational waves have long eluded direct detection due to their weak coupling with matter. Except in cases where the dynamics involves coherent bulk motion of masses larger than a few solar masses and/or speeds close to that of light, the amplitude of gravitational waves from astrophysical sources will not be high enough for Earth based antennas to detect them. Once detected, gravitational waves can be potentially used to measure astrophysical quantities such as the masses of compact stars in binary systems, their spins, equation of state of dense nuclear matter, as well as to test astrophysical models of the formation and evolution of binary systems, single pulsars, etc. Detection of gravitational waves will also be of cosmological importance since observation of signals from inspiralling binary systems would allow us to make an accurate estimate of the Hubble constant and measuring or setting limits on the stochastic background of gravitational waves can constrain models of the early Universe. Moreover, with the aid of gravitational waves it would be possible to test general relativity and other theories of gravity in the strongly nonlinear regime thus contributing to our knowledge of the fundamental laws of Nature. For a recent review on gravitational waves see Thorne [1,2].

The search for gravitational waves of cosmic origin has led to the development of long baseline optical Michelson type interferometers [3,4]. The effective baseline of these detectors must be of the order of 150 km. The physical length of the interferometer is reduced by using reflecting Fabry-Perot cavities of finesse $F \sim 50$–a few hundreds and physical length $L = 3$–4 km. The optical power is enhanced by a recycling system, and the surtension in the cavities is presently designed at about 10 kW. The mirrors are heavy silica blocks bearing dielectric reflective coatings. In order that the power recycling is efficient, the cavities must be highly reflective, which means that the coatings must have very low losses. With the current state-of-the-art, losses as low as a few ppm (10^{-6}) are planned [5,6], which results in about 10 mW dissipated in the coatings, and thus heating the substrates. The optical beam has a Gaussian profile and the corresponding heat source generates temperature

gradients. The temperature gradients cause a deformation of the substrate, and especially of its internal coated face interacting with the optical field. In the case of presently developed interferometers, the effect proves to be negligible [7,8]. However, for advanced instruments a special study should be undertaken showing the behavior of a resonant cavity with nonlinear effects, and especially with thermo-optical coupling.

The rest of the paper is organized as follows. In Sec.II we give a brief description of the problem of nonlinear effects in a resonant cavity highlighting the aim of the present study. We recall the methodology followed in an earlier work [11] for the study of static thermo-elastic effects in a high power laser cavity. The results of that study are extensively used in the present paper and we refer the interested reader to Hello and Vinet [11] for details. In Sec.III we take up the problem of thermal effects due to absorption of laser light by the coatings of the mirror and obtain an analytic expression for the temperature profile in the substrate of the mirror. Such an analysis is carried out for a single Fourier component of the fluctuating intra-cavity laser power and a general solution can be built from the solution obtained in this work. We then demonstrate that the exact analytical solution can be approximated by a very simple expression which shows that the thermal transfer function describing the temperature distribution in the substrate is 'identity' apart from an amplitude and a constant phase factor. This implies that the temperature profile on the mirror surface and within the substrate is identical to that of the light beam. Using the thermal transfer function we solve for the deformation of the substrate, in particular of the coating, in Sec.IV. Finally, in Sec.V we solve for the evolution of the phase of the intra-cavity light field in the presence of deformations induced by random fluctuations of the laser power. This is done by a heuristic derivation of the combined transfer function for the static and the time-dependent case describing the effect of the fluctuating laser field on the phase of the intra-cavity light, thus completing the full solution to the coupled thermo-elastic problem in high power laser cavities. In Sec.VI we give a summary of the results obtained in this study and discuss prospects for future work in this direction.

II. MOTIVATION AND BACKGROUND

In the next two Subsections we briefly discuss the relevance of the present study to the construction of the second generation gravitational wave interferometric antennas, the problems that have been addressed so far and how the results of previous work may be used to advantage in addressing more complex situations.

A. The Description of the Problem

We consider a resonant Fabry-Perot cavity in which the stored optical field can be strong enough to generate various nonlinear effects. Among these nonlinear effects, the thermo-elastic coupling will be studied here. In order to study the stability of this type of coupling, we shall assume that the stored power can vary in time. We shall first recall briefly the static solution found in the case of a constant Gaussian beam weakly dissipated by an isolated cylindrical mirror (axially symmetrical problem) because the mathematical tools employed in that study are essentially valid for the problem under consideration. Then we consider the case of a Gaussian beam having an oscillating power flux with a constant mean value. In all cases, we assume that the only heat losses are due to thermal exchange between the mirror and the surrounding vacuum vessel by radiation. In all cases we have to first address the temperature problem by solving the Fourier equation with the relevant boundary conditions, then the thermo-elastic problem : knowing the temperature field, find the displacement vector field by solving the thermo-elastic equations with the relevant boundary conditions. The distortion of the surface can be analyzed in terms of coupling of Hermite-Gauss modes. The second part of the problem is to study the behavior of a resonant cavity with a mirror having a time varying distortion. Finally, we shall obtain a first transfer function from the optical dynamical field to the distortion of the mirror, and a second transfer function from the distortion of the mirror to the optical amplitude. Combining the two transfer functions will give us some information on the behavior of a resonant cavity. It is, however, to be

noted that in this work we have not necessarily considered all nonlinear effects that might in principle lead to an instability. For instance, no effort is made in treating the radiation pressure effects which will obviously be of similar magnitude as the thermo-elastic effects and will be taken up in a future work. The main conclusion of this work is that even when very high powers $\sim$ 1 MWatt are stored the system does not show any instability or a chaotic behavior. This is certainly a welcome news for groups that have plans to build giant interferometric cavities.

B. The Static Solution

The static solution has been studied in detail by several authors (see eg. [9,10]) and more recently in two articles by some of us [11,12]. We recall here the general method. Owing to the cylindrical symmetry of the problem, due to the fact that we assume the light beam to coincide with the axis of the mirror, we can expand the temperature field, and the elastic deformations, in terms of Bessel functions as Dini series. This allows us to employ a trick found by Cutolo et al. [9] to solve the coupled equations for the radial and longitudinal deformations. In the static case, for large Silica mirrors, the characteristic time for the evolution of the temperature is $\sim$ 10's of hours and hence the evolution of the deformation is only quasi-static. This allows us to neglect inertial forces and the generation of acoustic waves in the substrate. An important result obtained in the static case is that the heating by absorption in the bulk of the substrate, as the laser beam traverses through it, is a factor of 5 less as compared to the case of heating by absorption in the coating for the same levels of absorbed power. The consequent aberrations produced in the former case are an order of magnitude lower as compared to those produced by thermal lensing. We make use of this result in the present work and neglect absorption of laser light in the bulk of the mirror. It was pointed out in those studies that though the beam transmitted through the mirror has negligible perturbations it might very well be that the reflected beam is affected to a higher degree. In this paper we take up the dynamical problem left undone in those works.

III. THE TEMPERATURE PROFILE IN THE MIRROR

In this Section we consider the thermal effects induced in the mirror by intra-cavity high power laser beam fluctuating at a certain fiducial frequency. The problem is first solved exactly with the proper boundary conditions. The exact solution is not of much utility in solving the thermo-elastic problem and hence we obtain an approximate, nevertheless accurate, solution to the problem and show that the two solutions match very well except when the power fluctuation time scale is too low. The most important result of this Section is that the temperature profile on the surface of the mirror is coincident with the optical beam profile.

A. The Heat Equation

The mirror is in the shape of a cylinder of radius a and thickness h and consists of a substrate, usually silica, and a high-quality reflective coating. In gravitational wave interferometers typically, $a \sim 0.1$ m and $h \sim 0.1$ m (for the input mirrors). The axis of the mirror is the z-axis and it is coated on the face at $z = 0$ (see Fig.1). The cavity lies along the positive z-axis with the other mirror (suitably curved) at $z = L$. The intra-cavity laser light is incident on the mirror at $z = 0$ which gets heated due to absorption in the coating. We neglect absorption in the substrate of the mirror. The mirror losses heat to its surroundings by radiation. We consider a time varying intensity profile $I(r)e^{-i\Omega t}$ with a single Fourier component at Ω; the general solution can be built up from these Fourier components (see Sec.V, especially Eq. (5.8)) since we shall linearize Stefan's laws which is justified as the rise in temperature of the substrate is very small. At frequencies $\Omega < 10$ rad s^{-1} the effects of a fluctuating laser power can be corrected with the aid of a transducer while for $\Omega > 10^3$ rad s^{-1} the thermal gradients and elastic deformations induced are negligible. Thus, we shall assume that 10 rad s^{-1} $< \Omega < 10^3$ rad s^{-1}. Also we assume axial symmetry so that I is a function only of the radial coordinate r. We will assume the intensity profile to be a

Gaussian so that $I(r)$ is a Gaussian with the maximum at $r = 0$ and standard deviation $w_0/2$, where w_0 is the waist of the beam. We assume that the change in the temperature of the mirror due to heating is small relative to the ambient temperature T_0. We have the following equation for the temperature distribution in the mirror which follows from heat conservation:

$$\rho C \frac{\partial T}{\partial t} = K \nabla^2 T, \tag{3.1}$$

where (for pure silica) ρ is the mass density (2202 kg m^{-3}), C is the specific heat capacity (745 J kg^{-1} K^{-1}) and K is the thermal conductivity (1.38 W m^{-1} K^{-1}). The Stefan's constant σ (5.67 $\times 10^{-8}$ W m^{-2} K^{-4}) enters into the boundary conditions and must be corrected for an emissivity factor since the mirror is not a black body. We assume an emissivity factor of 0.9. The boundary conditions imposing the balance of heat fluxes, consistent with the assumptions stated earlier, are:

$$-K \frac{\partial T}{\partial r}|_{r=a} = 4\sigma T_0^3 T|_{r=a}, \tag{3.2a}$$

$$-K \frac{\partial T}{\partial z}|_{z=-h} = 4\sigma T_0^3 T|_{z=-h}, \tag{3.2b}$$

$$-K \frac{\partial T}{\partial z}|_{z=0} = 4\sigma T_0^3 T|_{z=0} - \epsilon I(t,r). \tag{3.2c}$$

where, ϵ is the absorption coefficient which is typically about 10^{-5} down to 10^{-6}. In accordance with the assumption of small changes in the temperature relative to T_0, we have linearized the equations around the ambient temperature T_0 and in all these equations T represents the change in temperature from the ambient temperature.

We take the intensity $I(t,r)$ to be of the form $I(r)e^{-i\Omega t}$. The function $I(r)$ is the modulus square of the electric field. For a TEM_{00} mode, the profile is a Gaussian given by

$$I(r) = I(0)\exp(-2r^2/w_0^2), \tag{3.3}$$

where w_0 is the waist radius of the beam and we take it to be 0.02 m. The total power P in the beam is,

$$P = \int_0^{2\pi} \int_0^a I(r)\, r\, dr\, d\theta. \tag{3.4}$$

When the radius $a \gg w_0$, we have the relation,

$$P \simeq \frac{\pi w_0^2 I(0)}{2}. \tag{3.5}$$

We shall consider P of the order of 10 kW or even a MW. Then correspondingly the absorbed power is about 0.01 W to 1 W. As we shall see this entails an increase in temperature of a small fraction of a degree.

B. The Exact Solution

We obtain an exact solution to the heat equation by separating the variables. The solution is found in a series form. Assuming a time dependence for the temperature field of the form $e^{-i\Omega t}$, Eq. (3.1) takes the form

$$(i\Omega C\rho + K\nabla^2)T = 0. \tag{3.6}$$

Since axial symmetry is assumed, the convenient choice of coordinates is cylindrical coordinates. Assuming the solution in the form,

$$T = \sum_{n=1}^{\infty} \Theta_n(z) J_0(k_n r), \tag{3.7}$$

where J_0 is the zero-order Bessel function, we get $\Theta_n(z)$ satisfying the equation,

$$\Theta_n''(z) - u_n^2 \Theta(z) = 0. \tag{3.8}$$

Here $u_n^2 = k_n^2 - i\Omega\rho C/K$ and the prime denotes differentiation with respect to the argument. The constants k_n are determined by the radiative boundary condition (3.2a) at $r = a$ as follows. Let ξ_n be the n th root of the equation,

$$xJ_1(x) - \tau J_0(x) = 0, \tag{3.9}$$

where $\tau = 4\sigma T_0^3 a/K$; then $k_n = \xi_n/a$. For the parameters assumed and $T_0 \sim 300^0$ K, $\tau \sim 0.4$ and the first few ξ_n, $n = 1, 2, 3, 4, \ldots$, have the following approximate values: 0.85,

3.93, 7.07, 10.21, ... For large n the consecutive ξ_n differ approximately by π. The solution to Eq. (3.8) is,

$$\Theta_n(z) = \alpha_n \exp(u_n z/a) + \beta_n \exp(-u_n z/a), \tag{3.10}$$

where, the constants α_n and β_n are to be determined from the boundary conditions at $z = a$ and $z = -h$.

The functions $J_0(k_n r)$ have the property that they form a complete orthogonal set over the interval $[0, a]$ and satisfy the orthogonality relation,

$$\int_0^\infty J_0(k_m r) J_0(k_n r) r dr = \delta_{mn} \frac{\tau^2 + \xi_n^2}{2\xi_n^2} (J_0(\xi_n))^2 a^2. \tag{3.11}$$

Next, we expand $I(r)$ on the basis of $J_0(k_n r)$ as,

$$I(r) = \sum_{n=1}^{\infty} p_n J_0(k_n r), \tag{3.12}$$

where the coefficients p_n can be obtained by inverting the relation with the help of Eq. (3.11) and noting that $a \gg w_0$. Thus,

$$p_n \simeq \frac{P}{\pi a^2} \frac{\xi_n^2}{(\tau^2 + \xi_n^2)[J_0(\xi_n)]^2} \exp(-\xi_n^2 w_0^2/8a^2). \tag{3.13}$$

For our case where $a = 0.1$ m and $w_0 = 0.02$ m, the first few p_n's (in units of W m^{-2}) are as follows: $p_1 \sim 38$, $p_2 \sim 182$, $p_3 \sim 275$, $p_4 \sim 303$, $p_5 \sim 273$, ..., $p_{10} \sim 21$, $p_{17} \sim 10^{-3}$, ... The p_n exponentially fall off to zero as n increases further. With the above expression for $I(r)$, the boundary conditions (3.2a) and (3.2b) for $\Theta_n(z)$ become,

$$K\Theta_n'(-h) = 4\sigma T_0^3 \Theta_n(-h), \tag{3.14a}$$

$$-K\Theta_n'(0) = 4\sigma T_0^3 \Theta_n(0) - \epsilon p_n. \tag{3.14b}$$

These conditions give a pair of simultaneous equations for each value of n for α and β which then can be solved to yield $\Theta_n(z)$. Thus,

$$\Theta_n(z) = \frac{a}{K} \epsilon p_n \frac{(\tau + u_n) \exp[u_n(z+h)/a] - (\tau - u_n) \exp[-u_n(z+h)/a]}{(\tau + u_n)^2 \exp(u_n h/a) - (\tau - u_n)^2 \exp(-u_n h/a)}. \tag{3.15}$$

This gives the exact solution for the temperature profile within the mirror. Fig. 2 shows the plot of the temperature for various constant values of r as a function of z for a Watt of absorbed power. We notice that the temperature field is essentially nonzero close to the lit surface of the mirror and decays rapidly to zero away from the lit surface as well as towards the rim. The rise in temperature to a maximum of about $0.2°$ at the centre of the mirror at $z = 0$ is small as compared with the absolute temperature T_0. This suggests that an approximate solution may be possible. This is in fact so and we obtain such a solution in the next Subsection and we find that it is remarkably close to the exact one for $\Omega > 5$ rad s^{-1}.

C. The Approximate Solution

The basic reason that such an approximation exists is that we have two time scales in the problem one of which is much larger than the other:

1. The thermal time scale $t_{\text{therm}} \sim \rho C a^2/K$ which is typically several hours. Here we have $t_{\text{therm}} \sim 3$ hours.

2. The time scale of the intensity fluctuations t_{osc} which is $2\pi/\Omega$.

Secondly, most of the power is confined in the region of the waist w_0 of the beam and since $a \gg w_0$, the coefficients p_n fall off very rapidly to zero. For 1 W power absorbed, the maximum is $p_4 \sim 303$ W m^{-2} while $p_{15} \sim 0.1$ W m^{-2}, for this choice of parameters. We obtain an approximate solution when $\Omega t_{\text{therm}} \gg 1$ in a very simple and closed form as follows: Since the p_n decay very rapidly only the first few terms are important, say, up to $n \sim 15$. Now if $\Omega t_{\text{therm}} \gg \xi_{15}^2 \sim 2000$, then we can neglect ξ_n from Eq. (3.8). In other words, at low values of n, Ωt_{therm} dominates k_n^2 in Eq. (3.8), and for high values of n, low values of p_n make the contribution of $\Theta_n(z)$ insignificant. Thus, $\Theta_n(z)$ becomes independent of n, except for the factor p_n, and the series sums up to give essentially the intensity profile $I(r)$. Physically, this amounts to saying that there is no radiation from the rim of the mirror. Thus,

$$u_n \sim (1-i)/\delta, \tag{3.16}$$

where, δ is the 'skin depth' defined by,

$$\delta = \sqrt{\frac{2K}{\Omega C \rho}}. \tag{3.17}$$

Here $\delta \sim 4 \times 10^{-4}$ m for $\Omega = 10$ rad s^{-1}. Further, we neglect τ with respect to a/δ, which physically means negligible radiation from the surface $z = 0$, and we obtain a simple form for $\Theta_n(z)$,

$$\Theta_n(z) = \frac{\epsilon p_n \delta}{\sqrt{2}K} \exp\left[\frac{z}{\delta}(1-i) + i\frac{\pi}{4}\right]. \tag{3.18}$$

The final result is that the p_n's combine with the $J_0(k_n r)$ in Eq. (3.7) to yield the intensity profile $I(r)$ and we obtain,

$$T(t,r,z) = \frac{\epsilon I(r)\delta}{\sqrt{2}K} \exp\left[\frac{z}{\delta} - i\left(\frac{z}{\delta} - \frac{\pi}{4} + \Omega t\right)\right]. \tag{3.19}$$

This solution agrees very well with the exact solution for sensible choice of the parameters, for example, for $\Omega = 10$ rad s^{-1}. The approximation in fact improves at higher frequencies.

IV. THE THERMO-ELASTIC PROBLEM

In this Section we address the problem of computing the deformations produced in the substrate and on its reflective coating. Thermo-elastic equations together with the boundary conditions are introduced in Sec.IV A. To obtain a closed form solution we use the approximate form of the temperature field derived earlier. This facilitates to express the solution to the thermo-elastic equations, in Sec.IV B, in a manner similar to that followed in the Sec.III by employing Bessel series expansion. We end this Section by computing the maximum and average deformations produced in Sec.IV C, and the concomitant phase shift induced in the light beam, and show that even when the power stored in the intra-cavity is as high as 1 MW the largest deformation is less than one part in 10^4 of the wavelength of infra-red laser used in gravitational wave interferometric detectors.

A. Thermo-elastic equations

Since the temperature changes are basically confined in a thin region close to the lit surface of the mirror, the thermo-elastic forces appear like a boundary condition at the surface $z = 0$. The varying temperature produces varying deformation near this surface and gives rise to acoustic waves within the mirror. But we will principally be interested in the deformation of the surface $z = 0$ because it is the deformation of this surface that couples to the intracavity light field. We again proceed by Fourier analysis.

The strain tensor E_{ik} in terms of the displacement vector $\mathbf{u}$ is,

$$E_{ik} = \frac{1}{2}\left(\frac{\partial u_i}{\partial x_k} + \frac{\partial u_k}{\partial x_i}\right). \tag{4.1}$$

in Cartesian coordinates. The stress tensor Θ_{ik} for homogeneous and isotropic medium in which there is a temperature field T is given by [13],

$$\Theta_{ik} = (-\nu T + \lambda E)\delta_{ik} + 2\mu E_{ik}, \tag{4.2}$$

where, μ, λ are the Lamé coefficients, ν is the stress temperature modulus and E is the trace of E_{ik}. For pure silica $\mu = 3.13 \times 10^{10}$ J m^{-3}, $\lambda = 1.56 \times 10^{10}$ J m^{-3} and $\nu = 5.91 \times 10^{4}$ J m^{-3} K^{-1}.

Since we assume axial symmetry, we choose cylindrical coordinates in which the strain and the stress tensors take the following form:

$$E_{rr} = \frac{\partial u_r}{\partial r},\ E_{\phi\phi} = \frac{u_r}{r},\ E_{zz} = \frac{\partial u_z}{\partial z},\ E_{rz} = \frac{1}{2}\left(\frac{\partial u_r}{\partial z} + \frac{\partial u_z}{\partial r}\right), \tag{4.3}$$

$$\Theta_{rr} = -\nu T + \lambda E + 2\mu E_{rr}, \tag{4.4a}$$

$$\Theta_{\phi\phi} = -\nu T + \lambda E + 2\mu E_{\phi\phi}, \tag{4.4b}$$

$$\Theta_{zz} = -\nu T + \lambda E + 2\mu E_{zz}, \tag{4.4c}$$

$$\Theta_{rz} = 2\mu E_{rz}. \tag{4.4d}$$

The dynamical equations are [13],

$$\frac{\partial \Theta_{rr}}{\partial r} + \frac{\partial \Theta_{rz}}{\partial z} + \frac{\Theta_{rr} - \Theta_{\phi\phi}}{r} = \rho \frac{\partial^2 u_r}{\partial t^2}, \tag{4.5a}$$

$$\frac{\partial \Theta_{rz}}{\partial r} + \frac{\partial \Theta_{zz}}{\partial z} + \frac{\Theta_{rz}}{r} = \rho \frac{\partial^2 u_z}{\partial t^2}. \tag{4.5b}$$

These equations have to be solved together with the boundary conditions,

$$\Theta_{zz}|_{z=0} = \Theta_{zz}|_{z=-h} = \Theta_{rz}|_{z=0} = \Theta_{rz}|_{z=-h} = \Theta_{rz}|_{z=a} = \Theta_{rr}|_{r=a} = 0. \tag{4.6}$$

The corresponding equations for the displacement vector components u_r and u_z are second order coupled but linear differential equations. Assuming the time dependence for $\mathbf{u}$ as $e^{-i\Omega t}$, the equations are,

$$(\lambda + 2\mu)\frac{\partial^2 u_r}{\partial r^2} + (\lambda + \mu)\frac{\partial^2 u_z}{\partial r \partial z} + \mu \frac{\partial^2 u_r}{\partial z^2} + (\lambda + 2\mu)\frac{\partial}{\partial r}\left(\frac{u_r}{r}\right) + \rho u_r \Omega^2 = \nu \frac{\partial T}{\partial r}, \tag{4.7a}$$

$$(\lambda + 2\mu)\frac{\partial^2 u_z}{\partial z^2} + (\lambda + \mu)\frac{\partial^2 u_r}{\partial r \partial z} + \mu \frac{\partial^2 u_z}{\partial r^2} + \frac{(\lambda + \mu)}{r}\frac{\partial u_r}{\partial z} + \left(\frac{\mu}{r}\right)\frac{\partial u_z}{\partial r} + \rho u_z \Omega^2 = \nu \frac{\partial T}{\partial z}. \tag{4.7b}$$

B. Solution to the thermo-elastic problem

To solve the thermo-elastic equations we follow the method of suggested by Cutolo et al. [9] (see also, Hello and Vinet [12]). First we expand the u_r, u_z and T in a Bessel function series, in terms of $J_0(k_n r)$ for u_z and T, and $J_1(k_n r)$ for u_r. Thus, we write,

$$u_r = \sum_{m=1}^{\infty} A_m(z) J_1(k_m r), \tag{4.8a}$$

$$u_z = \sum_{m=1}^{\infty} B_m(z) J_0(k_m r), \tag{4.8b}$$

$$T = \sum_{m=1}^{\infty} T_m(z) J_0(k_m r), \tag{4.8c}$$

where the k_m could be chosen to be the same as before (cf. Eq. (3.9)). However, this choice is not unique and we are free to choose some other sequence of numbers k_m which produce an orthogonal basis of functions. The k_m chosen earlier are tied to the thermal

problem. They suffice here as well and shall use them in the analysis that follows. We can immediately obtain $T_m(z)$ from Eqs. (3.12) and (3.19). Comparing terms for a given m, we have,

$$T_m(z) = \alpha_m e^{\beta z}, \quad \alpha_m = p_m \frac{\delta}{\sqrt{2}K} e^{i\pi/4}, \quad \beta = \frac{1-i}{\delta}. \tag{4.9}$$

For A_m and B_m we get two coupled equations with forcing terms in T_m. Thus,

$$(\mu+\lambda)(B_m'' + k_m A_m') + \mu(B_m'' - k_m^2 B_m) + \rho\Omega^2 B_m = \nu \frac{\partial T_m}{\partial z}, \tag{4.10a}$$

$$(\mu+\lambda)k_m(B_m' + k_m A_m) - \mu(A_m'' - k_m^2 A_m) - \rho\Omega^2 A_m = k_m \nu T_m, \tag{4.10b}$$

where the prime denotes differentiation with respect to z. Defining $U_m = A_m' + k_m B_m$, we obtain an equation for U_m,

$$U_m'' + \left(\frac{\Omega^2}{c_2^2} - k_m^2\right) U_m = 0, \tag{4.11}$$

where, $c_2 = \sqrt{\mu/\rho}$ is the velocity of the transverse sound wave. For silica, $c_2 \sim 3770$ m s^{-1}. For the range of Ω we are considering $\Omega < 1000$ rad s^{-1}, and we have $\frac{\Omega^2}{c_2^2} \ll k_m^2$ and hence we ignore it in the calculations that follow. This amounts to neglecting the inertial term. Thus, solving Eq. (4.11), we have,

$$A_m' + k_m B_m = 2k_m(R_m \cosh k_m z - S_m \sinh k_m z), \tag{4.12}$$

where, R_m and S_m are constants to be determined from the boundary conditions. We now solve Eqs. (4.10b) and (4.12) simultaneously. Eliminating $B_m(z)$ between these equations we obtain an equation for $A_m(z)$,

$$A_m'' - k_m^2 A_m = -\frac{k_m \nu \alpha_m}{\lambda+\mu} e^{\beta z} + 2\eta k_m^2 (R_m \sinh k_m z - S_m \cosh k_m z), \tag{4.13}$$

where, $\eta = (\mu+\lambda)/(2\mu+\lambda)$. The solution to Eq. (4.13) is,

$$A_m(z) = P_m \cosh k_m z + Q_m \sinh k_m z + \eta k_m z (R_m \cosh k_m z - S_m \sinh k_m z) - \gamma_{2m} e^{\beta z}, \tag{4.14}$$

where,

$$\gamma_{2m} = \frac{k_m \nu \alpha_m}{(\lambda + 2\mu)(\beta^2 - k_m^2)}. \tag{4.15}$$

Then $B_m(z)$ follows from Eq. (4.12),

$$B_m(z) = -P_m \sinh k_m z - Q_m \cosh k_m z + (2-\eta)(R_m \cosh k_m z - S_m \sinh k_m z)$$
$$+\gamma_{1m} e^{\beta z} - \eta k_m z (R_m \sinh k_m z - S_m \cosh k_m z), \tag{4.16}$$

where, $\gamma_{1m} = \beta \gamma_{2m}/k_m$. These give the solutions to the equations with four sets of arbitrary constants P_m, Q_m, R_m and S_m which must be determined via the boundary conditions at the surface of the mirror. We make use of the boundary conditions listed in Eq. (4.6). The first four boundary conditions at the two flat surfaces of the mirror give the following conditions on A_m and B_m at $z = 0$ and $z = -h$:

$$A_m' - k_m B_m = 0, \tag{4.17a}$$

$$-\nu T_m + \lambda k_m A_m + (\lambda + 2\mu) B_m' = 0. \tag{4.17b}$$

The first follows from the vanishing of Θ_{rz} and the second from Θ_{zz} at the flat surfaces. Together with (4.12) the first condition yields the important relation,

$$B_m(0) = R_m. \tag{4.18}$$

This means that we need only solve for R_m in order to get the deformation of the surface at $z = 0$. In other words, the deformation of the reflective coating of the substrate is given by

$$u_z(z=0) = \sum_{m=1}^{\infty} R_m J_0(k_m r). \tag{4.19}$$

The boundary conditions (cf. Eq. (4.6)) give four sets of simultaneous equations for the constants P_m, Q_m, R_m and S_m. Since the equations do not mix the index m, we drop this index for brevity and also write $x = k_m h$. Thus,

$$Q + (\eta - 1)R = \gamma_1, \tag{4.20}$$

$$-P \sinh x + Q \cosh x + R(\eta x \sinh x + (\eta - 1)\cosh x) + S((\eta - 1)\sinh x + \eta x \cosh x) = 0, \tag{4.20}$$

$$P + S = \gamma_2, \tag{4.20}$$

$$P \cosh x - Q \sinh x - R(\eta x \cosh x - \sinh x) + S(\cosh x - \eta x \sinh x) = 0. \tag{4.20}$$

These equations can be easily solved for P, Q, R and S to yield the displacement vector. However, we are only interested in the deformation of the surface at $z = 0$. According to Eq. (4.19) we need only compute R. Solving,

$$R = \frac{\zeta_1 \sinh x - \zeta_2(x + \sinh x \cosh x)}{\sinh^2 x - x^2}, \tag{4.21}$$

where, introducing the index m again,

$$\zeta_{1m} = \eta^{-1}\gamma_{1m} = \frac{\beta\nu\alpha_m}{(\mu+\lambda)(\beta^2 - k_m^2)}, \tag{4.22a}$$

$$\zeta_{2m} = \eta^{-1}\gamma_{2m} = \frac{\nu\alpha_m k_m}{(\mu+\lambda)(\beta^2 - k_m^2)}. \tag{4.22b}$$

For the parameters we have chosen, again only the first few terms, say about a dozen, matter because $\alpha_m \propto p_m$. But in that case, $\beta^2 \gg k_m^2$ which in turn implies that $\zeta_{2m} \ll \zeta_{1m}$. Thus, we neglect ζ_{2m} from (4.21) and obtain a more simplified form for $\zeta_{1m} \sim \nu\alpha_m/\beta(\mu+\lambda)$. The final result is that

$$u_z|_{\text{surface}} = i\left(\frac{\nu}{\mu+\lambda}\right)\frac{\delta^2}{2K}\left[I(r) + \sum_{m=1}^{\infty} p_m q_m J_0(k_m r)\right], \tag{4.23}$$

where,

$$q_m = \frac{(k_m h)^2}{\sinh^2 k_m h - (k_m h)^2}. \tag{4.24}$$

For $h = 0.1$ m, $k_1 h \sim 0.85$, $k_2 h \sim 3.93, \ldots$, and the q_m are practically zero except for $q_1 \sim 3.76$. So only the first term is significant in the series in Eq. (4.23). Moreover, in the region of the beam $r \sim w_0$ and $J_0(k_1 r)$ is constant equal to unity. Thus the square bracket collapses to $[I(r) + p_1 q_1]$ essentially and the expression for u_z at the surface $z = 0$ is considerably simplified.

$$u_z(r, \Omega) = i\frac{\nu}{\mu+\lambda}\frac{f(r)}{\rho C \Omega}, \tag{4.25}$$

where, $f(r) = \epsilon(I(r) + p_1 q_1)$.

C. Deformation of the mirror and phase shift

The maximum displacement is at $r = 0$. This may be easily computed for a given absorbed power ϵP. Let us assume $\epsilon P = 1$ W. Then, we have, $\epsilon I(0) = 2\epsilon P/\pi w_0^2 \sim 1592$ W m^{-2} and $\epsilon p_1 \sim 38$ W m^{-2} which gives $f(0) \sim 1734$ W m^{-2}. Thus, $|u_z(0,\Omega)| \sim 1.33 \times 10^{-9}$ m Ω^{-1}. This is the displacement at the centre of the mirror per Watt of absorbed power and it is a tiny fraction of the wavelength of laser. In Fig.3 we plot the deformation $|u_z(r,\emptyset)|$ as a function of r for $\Omega = 10$ rad s^{-1} and 1 Watt of absorbed power.

We similarly compute the average displacement of the surface $z = 0$ averaged over the intensity profile. This is needed in the next Section where we investigate the effect of the deformation on the light intensity. For this purpose we need the normalized Φ_{00} mode;

$$\Phi_{00} = \left(\frac{2}{\pi w_0^2}\right)^{\frac{1}{2}} \exp(-r^2/w_0^2), \tag{4.26}$$

which satisfies, $\int_{\mathcal{A}} |\Phi_{00}|^2 dS \simeq 1$ where the integral is over the area of the mirror surface $\mathcal{A}$. The average displacement is given by

$$\langle u_z \rangle (\Omega) = \int_{\mathcal{A}} u_z |\Phi_{00}|^2 dS. \tag{4.27}$$

This gives for 1 Watt of absorbed power,

$$\langle u_z \rangle (\Omega) \sim 0.72i \times 10^{-9}\ \Omega^{-1}\text{m}. \tag{4.28}$$

The phase ψ corresponding to this deformation is obtained by multiplying this average displacement by twice the wave number $k = 2\pi/\lambda$ of the laser light. Thus we have,

$$\psi(\Omega) = 2k \langle u_z \rangle (\Omega). \tag{4.29}$$

The Nd-Yag laser has wavelength $\lambda \sim 10^{-6}$ m (in the infra red). Thus, for this wavelength we obtain,

$$\psi(\Omega) \sim 0.9i \times 10^{-2}\Omega^{-1}. \tag{4.30}$$

This is the phase de-tuning obtained per Watt of absorbed power. In the next Section we turn to the effect of this deformation on the intra-cavity field.

V. THE OPTICAL COUPLING

In this Section we estimate the effect of the deformation on the intra-cavity light field. The effect of the deformation is to basically de-tune the cavity. We give below a time dependent treatment of this problem and connect it in an empirical way to the static solution earlier obtained by Hello and Vinet [12]. We consider the situation when the frequency of oscillation is much smaller than the free spectral range of the cavity. For instance, the free spectral range of the cavity for the VIRGO detector is $\sim$ 50 kHz. corresponding to an arm-length of 3 km. For smaller cavities the free spectral range is even larger. In this case we are able to obtain a differential equation for the phase ψ. We find that at least in this regime there are *no oscillations* in the light intensity.

We consider a cavity as shown in the Fig. 4. The amplitude of the input electric field is assumed to be a constant equal to A. The amplitude of the intra-cavity field $B(t)$ is assumed to vary slowly relative to the laser frequency $\sim 2.8 \times 10^{14}$ Hz. The intra-cavity light field satisfies the following self-consistent equation:

$$B(t) = \sqrt{T}A + Re^{i(\phi_0+\psi)}B(t-\tau), \tag{5.1}$$

where, $\sqrt{T}$ = the amplitude transmitivity of the corner mirror M_1, $R = r_1 r_2$ = is the product of the reflectivities of the corner mirror M_1 and and end mirror M_2, ϕ_0 is the de-tuning of the cavity, $\tau = 2L/c$, is the round trip travel time within the cavity and ψ is phase de-tuning due to the deformation. We neglect τ in our calculations since ($\Omega\tau \ll 1$). Then we may solve for $B(t)$,

$$B(t) = \frac{\sqrt{T}A}{1 - Re^{i(\phi_0+\psi)}}. \tag{5.2}$$

The intra-cavity power $P(t)$ is then just the square of the modulus of $B(t)$,

$$P(t) = \frac{T|A|^2}{|1 - Re^{i(\phi_0+\psi)}|^2}. \tag{5.3}$$

By including a factor of ϵ we may relate this power to the phase shift ψ suffered due to thermo-elastic effects. Thus, from Eq. (4.30) we obtain in the Fourier space,

$$\psi(\Omega) = i\alpha\epsilon\frac{P(\Omega)}{\Omega}, \tag{5.4}$$

where, $\alpha = 0.9 \times 10^{-2}\mathrm{J}^{-1}$. This equation is valid when the oscillation time scale is much smaller than the thermal time scale. We may, however, combine this with the static solution of Hello and Vinet [12] in a heuristic manner. We do this by defining a combined transfer function. In the static case,

$$\psi(0) = \alpha(0)\epsilon P(0), \quad \alpha(0) = \frac{4\pi}{\lambda}u_z(0) \sim 2.4\mathrm{W}^{-1}. \tag{5.5}$$

Further, we define a knee frequency Ω_0 by,

$$\Omega_0 = \frac{\alpha}{\alpha(0)}\mathrm{rad\ s}^{-1}. \tag{5.6}$$

In our case $\Omega_0 \sim 40$ mHz. We define the combined transfer function $Y(\Omega)$ by,

$$\psi(\Omega) = Y(\Omega)P(\Omega), \quad Y(\Omega) = \frac{\alpha\epsilon}{\Omega_0 - i\Omega}. \tag{5.7}$$

This transfer function goes to the expected limits: For $\Omega = 0$ we get the static transfer function, while for $\Omega \gg \Omega_0$ we obtain the transfer function given by (5.4) and thus the combined transfer function smoothly goes over to the static limit and we are quite justified in using the above equation for describing what happens in the most general case. In Fig.5 we plot the combined transfer function given by Eq. (5.7).

In order to ascertain the temporal behavior of the phase $\psi(t)$ we derive a differential equation as follows. First note that,

$$\psi(t) = \int_{-\infty}^{\infty} Y(\Omega)P(\Omega)e^{-i\Omega t}d\Omega. \tag{5.8}$$

By differentiating this expression with respect to t we get after some algebra, the differential equation for $\psi(t)$. Thus,

$$\frac{d\psi(t)}{dt} = -\Omega_0\psi(t) + \alpha\epsilon P(t). \tag{5.9}$$

We recover the static case in the limit $\frac{d\psi}{dt} \longrightarrow 0$; that is, we recover Eq. (5.5). In terms of ψ the equation can be written in the form,

$$\frac{d\psi}{dt} = g(\psi), \quad g(\psi) = -\Omega_0\psi + \frac{\alpha\epsilon T|A|^2}{1+R^2-2R\cos(\psi+\phi_0)}. \tag{5.10}$$

This equation may be put into a more convenient form:

$$\frac{d\psi}{d(\Omega_0 t)} = -\psi + \frac{a}{b-\cos(\psi+\phi_0)}, \tag{5.11}$$

where, $a = \frac{\alpha\epsilon T|A|^2}{2R\Omega_0}$, $b = \frac{1+R^2}{2R}$. Note that since $R \leq 1$, $b \geq 1$ and for $b > 1$ we obtain a stable solution. In Fig.6 we plot the evolution of the phase ψ. The plot clearly demonstrates that there is no instability whatsoever; within a few tens of the power fluctuation time-scale the phase reaches 99% of its asymptotic value. For small values of ψ we can expand the cosine and retain only first order terms in ψ. Then for the case of $\phi_0 = 0$, we can integrate (5.11) to obtain,

$$\Omega_0 t = \int_0^{\psi} \frac{(b-1)}{a-(b-1)\psi} d\psi, \tag{5.12}$$

which yields,

$$\psi \sim \frac{a}{b-1}\left(1 - e^{-\Omega_0 t}\right). \tag{5.13}$$

If we assume the following values for the parameters: $P_{\text{intra-cavity}} \sim T|A|^2/(1-R)^2, R \sim 0.94, \epsilon \sim 10^{-6}$ then, $a \sim 10^{-4}$ to $\sim 10^{-5}$ and $b \sim 1.002$. Then $a/(b-1) \sim 10^{-2}$ and ψ reaches this value asymptotically. This approximate solution agrees well with the numerical solution plotted in Fig.6.

Asymptotically, we obtain the static solution. There does not appear to be any instability or oscillation in the power within this model at frequencies ≥ 1 Hz, when ψ is assumed to be small. Perhaps, one must look at the problem non-perturbatively to obtain a physically different behavior.

VI. CONCLUSIONS

Laser interferometric gravitational wave antennas acquire their high sensitivity to detect radiation from cosmological distances by employing very long Fabry-Perot cavities of effective

length $\sim$ 150 km and laser beams of high power $\sim$ 10 kW–1 MW. Due to the absorption of radiation and the consequent heating the reflective coating of the mirror gets deformed, in turn altering the resonance condition of the cavity. In addition to this thermo-elastic deformation, and the associated instabilities, there are other sources of concern such as deformations and displacements of the mirrors due to radiation pressure, warping of the reflective coating due to its differential expansion with respect to the substrate, thermal vibrations of the mirror, etc. All these effects are in principle coupled and when intense laser beams exist in the cavity the problem is highly nonlinear. For the first generation of gravitational wave interferometers these nonlinearities are possibly negligible but we cannot hope for the same in future generations of interferometers. In this study we have addressed one of the issues, namely, the thermo-elastic effects and how they back react on the resonance condition of the cavity. Other issues, notably the radiation pressure-driven instabilities and the warping of the mirror, will be taken up in a future work. We have implicitly assumed in this work that the system is controlled by a servo system which drives the cavity into resonance on times scales $\sim$ 100 ms and hence we do not consider thermo-elastic effects on such time scales. The bottom line of this work is that under the physically reasonable assumptions, such as the one stated above, we do not see the development of any instability given that there is a transducer that takes care of motions occurring on large time scales.

Starting with the heat conservation equation (Sec.III) we solve for the temperature profile in the substrate and on its reflective coating in the presence of a fluctuating light field in the cavity. We show that there exists an approximate, but reasonably accurate, solution to the thermal distribution, derived based on the assumption of negligible radiation from the rim of the substrate, which shows that the profile of the temperature on the mirror is identical to that of the light beam. With the aid of this approximate solution we solve for the thermo-elastic deformations of the substrate, in particular of its reflective coating, and show that, for time scales involved, the deformations are a tiny (10–4) fraction of the wavelength of the laser (Sec.IV). With a knowledge of the thermo-elastic deformations, and the solution to the static problem obtained by Hello and Vinet [11,12], we construct a transfer function

for the phase offset induced in the resonance condition due to the coupling of the light field with thermo-elastic deformations. This, then allows us to obtain a differential equation for the phase offset that is solved numerically (and analytically in the perturbative limit) which shows no anomalous behavior in the frequency range 1 Hz–10 kHz.

The results of this work are some what unexpected since the problem is nonlinear and coupled. Generally, such systems do show some kind of instability or the other. It may be that not all effects that will be present in a realistic system are not being considered and hence we are unable to locate any chaotic behavior.

Acknowledgements

This work was supported by a grant provided by the *Indo-French Centre for the Promotion of Advanced Research (Centre Franco-Indien Pour La Promotion De La Recherche Avancee)* under the project 1001-1. The authors greatfully acknowledge the Centre for its encouragement.

REFERENCES

[1] K.S. Thorne, in *300 Years of Gravitation*, S.W. Hawking and W.Israel (eds.), (Cambridge Univ. Press, 1987).

[2] K.S. Thorne, *Gravitational Waves,* to be published in *Proceedings of the Snowmass 95 Summer Study on Particle and Nuclear Astrophysics and Cosmology,* E.W. Kolb and R.Peccei (eds.), (World Scientific, Singapore).

[3] C. Bradaschia *et. al.*, Nucl. Instrum. Methods Phys. Res., Sect A 518 (1990).

[4] A. Abramovici *et. al.*, Science **256,** 325 (1992).

[5] G. Rempe, R.J. Thompson, H.J. Kimble and R.Lalezari, Opt. Lett., **17,** 363 (1992).

[6] N. Uehara, et al., Opt. Lett., **20,** 530 (1995).

[7] W. Winkler, K. Danzmann, A. Rudiger and R. Schilling, Phys. Rev. A **44,** 7022 (1991).

[8] P. Hello and J-Y. Vinet, Phys. Lett. A **178,** 351 (1993).

[9] A. Cutolo, P. Gay and S. Solimeno, Opt. Acta, **27,** 1105 (1980).

[10] C.J. Myers and R.C. Allen, Appl. Opt., **24,** 1933 (1985).

[11] P. Hello and J-Y. Vinet, J. Phys. France, **51,** 1267 (1990).

[12] P. Hello and J-Y. Vinet, J. Phys. France, **51,** 2243 (1990).

[13] A.D. Kovalenko, Thermoelasticity – Basic theory and applications (Walters-Noordhoff, Groningen, 1969).

FIGURES

FIG. 1. Schematic diagram of the substrate of the mirror and its coating heated by the intra-cavity laser beam.

FIG. 2. Temperature profile as a function of the radial coordinate r and longitudinal coordinate z. Except close to the mirror surface and at the centre of the beam the rise in temperature is negligible. The radius of the mirror and the thickness of the substrate are 10 cm but the plot is only shown for a portion of the mirror.

FIG. 3. Plot of the thermo-elastic deformation of the reflective coating of the substrate $u_z(r, 0)$.

FIG. 4. Schematic diagram of the Fabry-Perot cavity showing the input and the intra-cavity field and the coupling of the cavity to thermo-elastic deformation.

FIG. 5. The transfer function for the phase shift induced in the cavity due to the thermo-elastic coupling of the light field.

FIG. 6. Development of the phase offset induced in the cavity due to thermo-elastic deformation. The phase gradually increases and within a few 10's of the fluctuation time-scale Ω^{-1} it reaches it attains 99% of its asymptotic value and we do not see any instability.

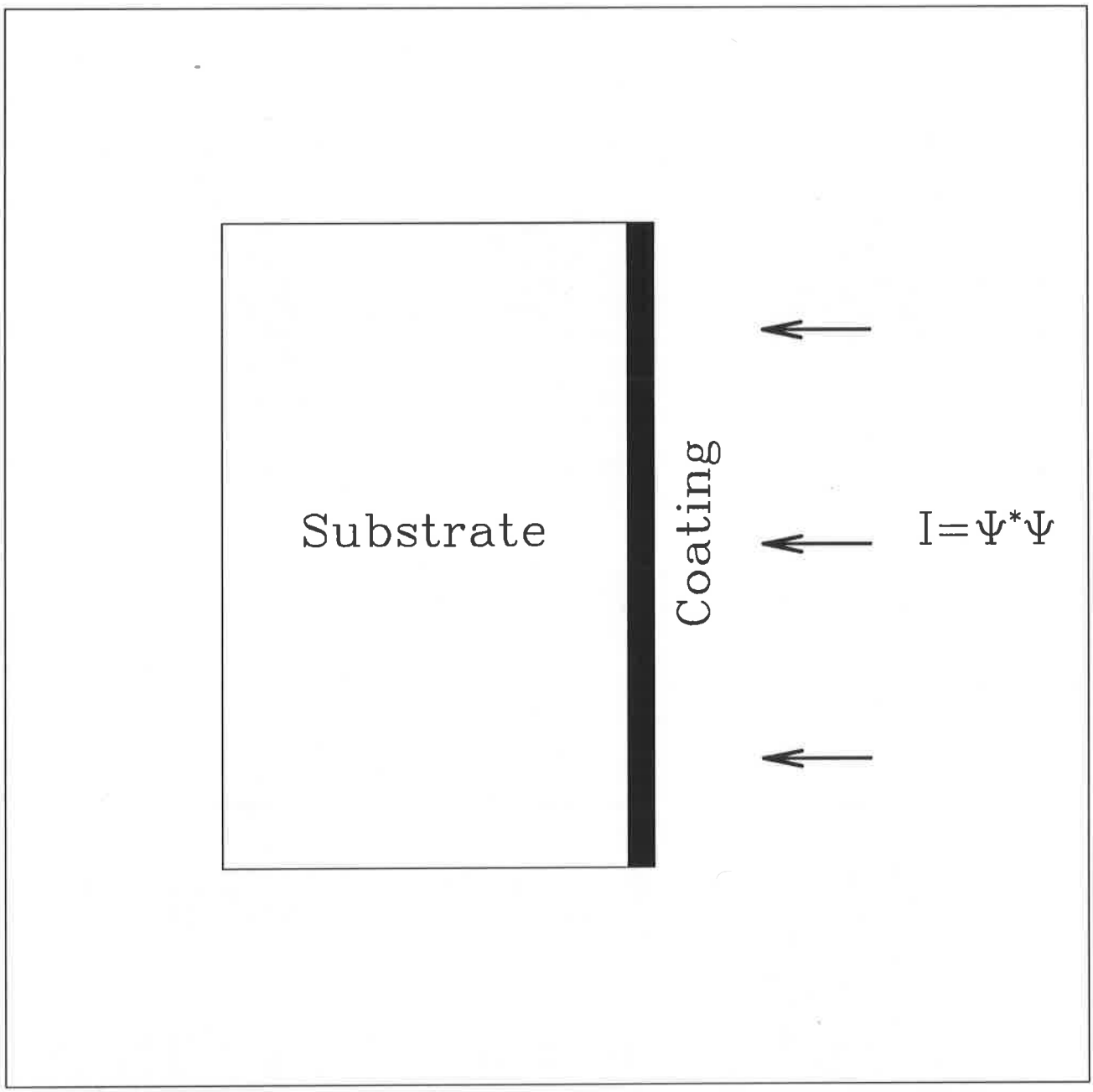

Fig 1

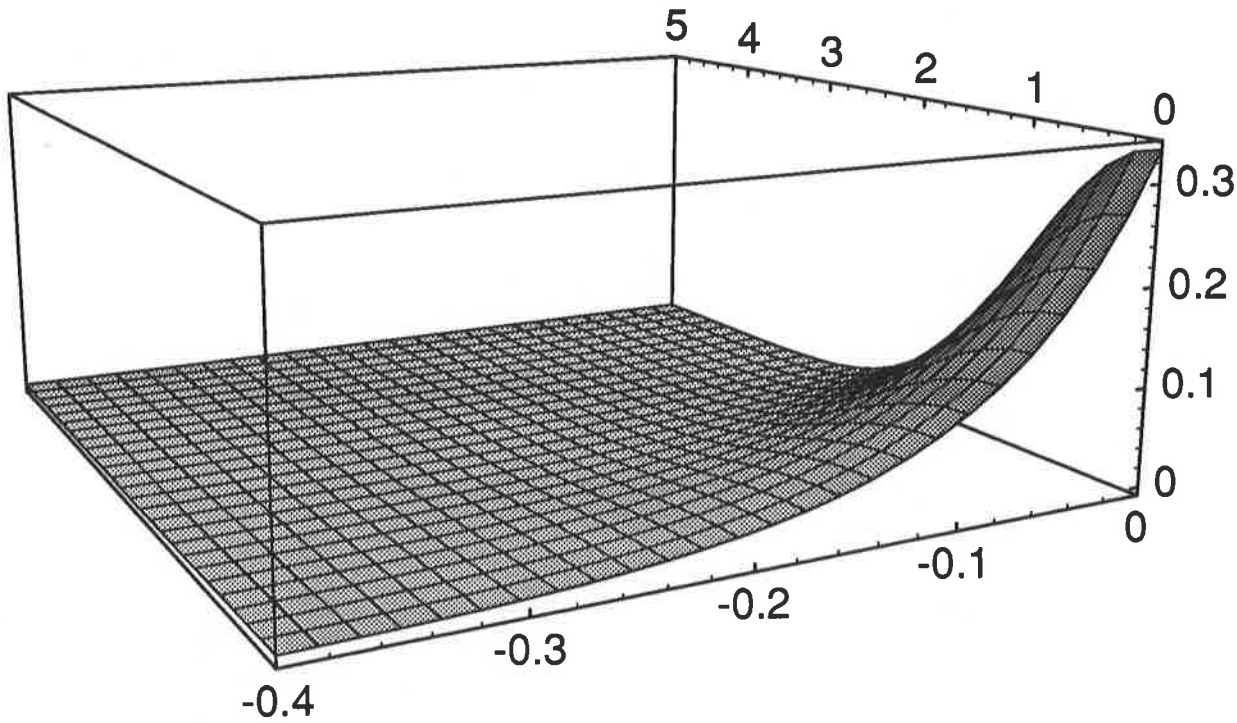

Fig 2

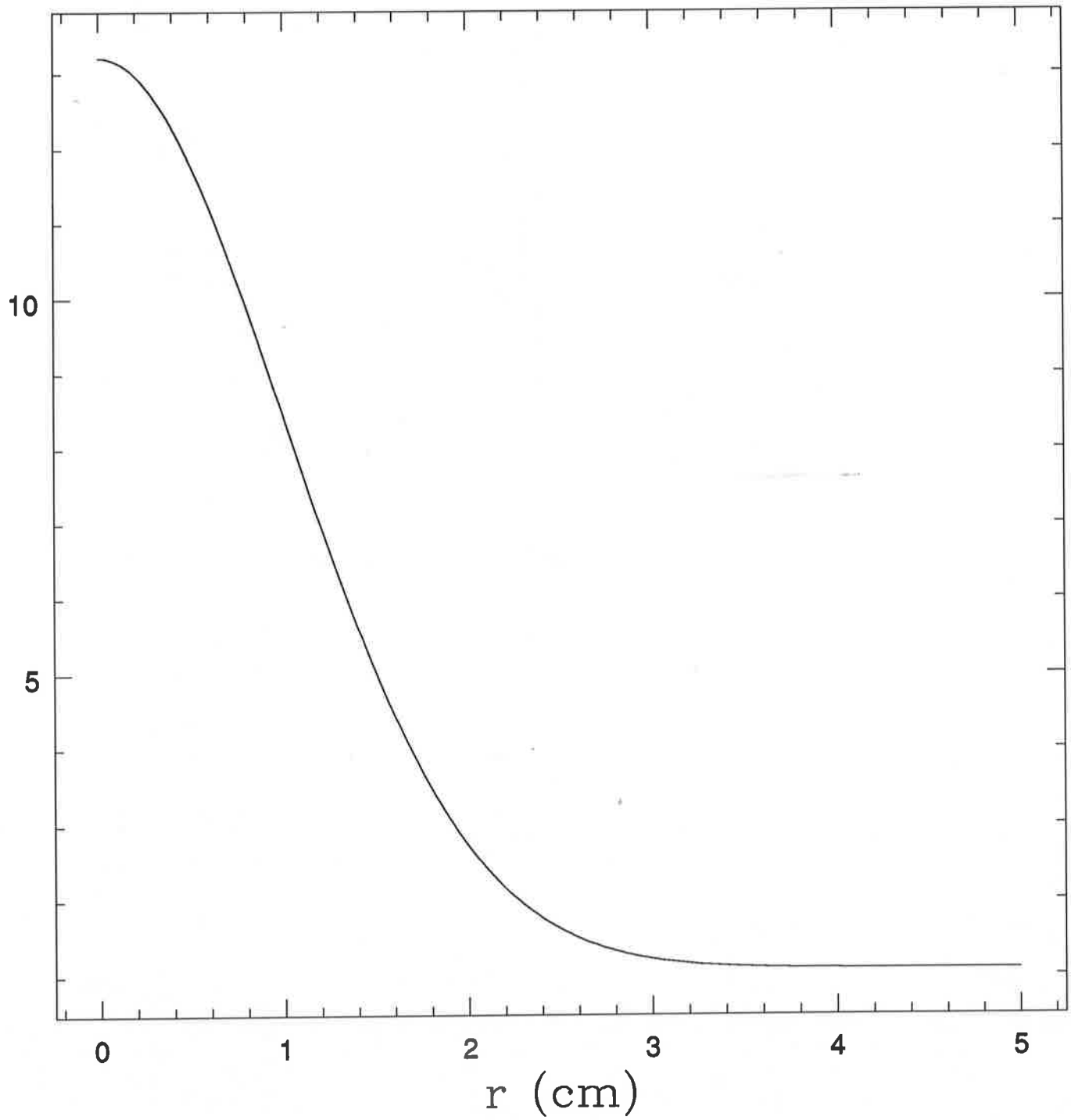

Fig 3

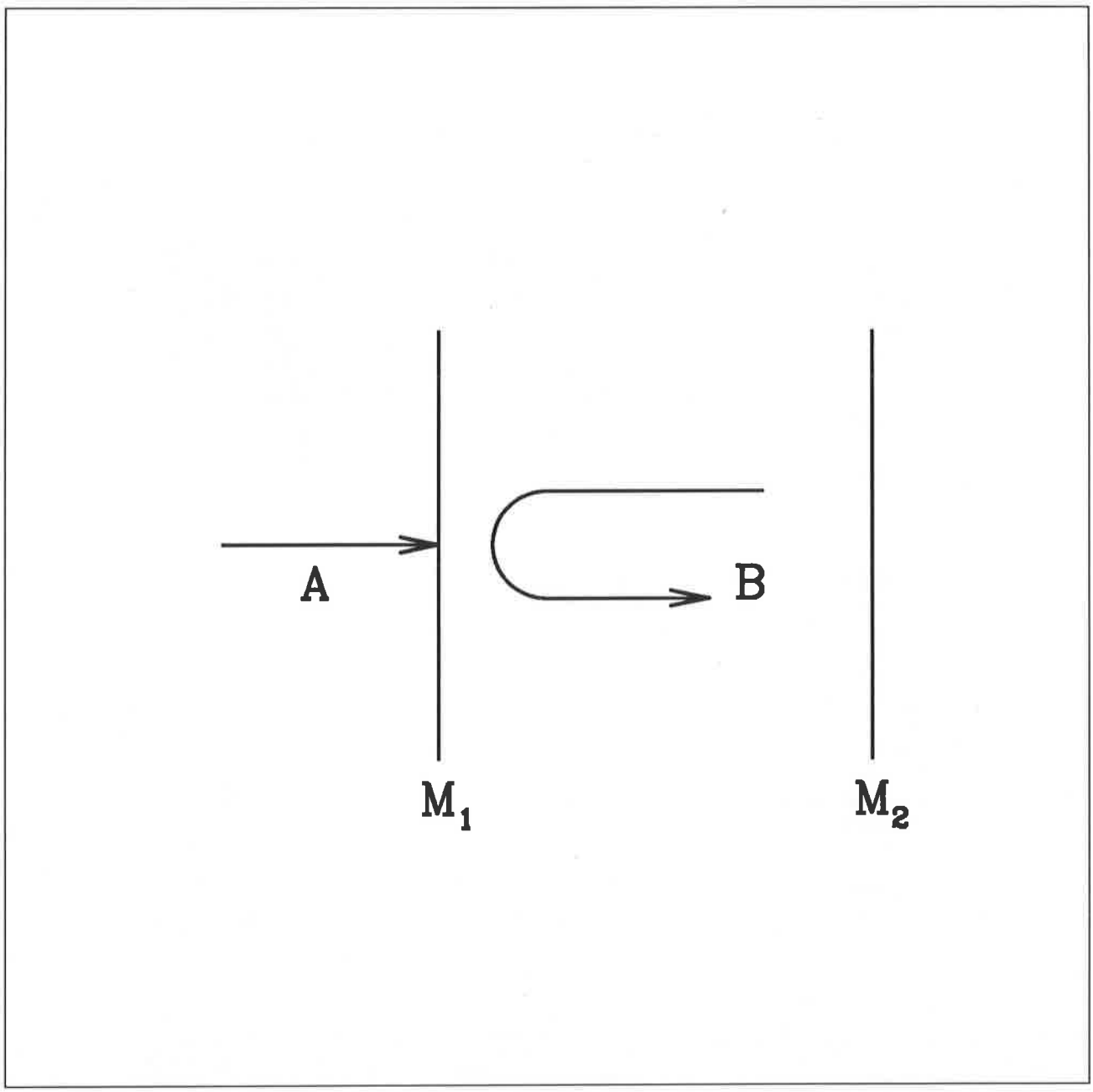

Fig 4

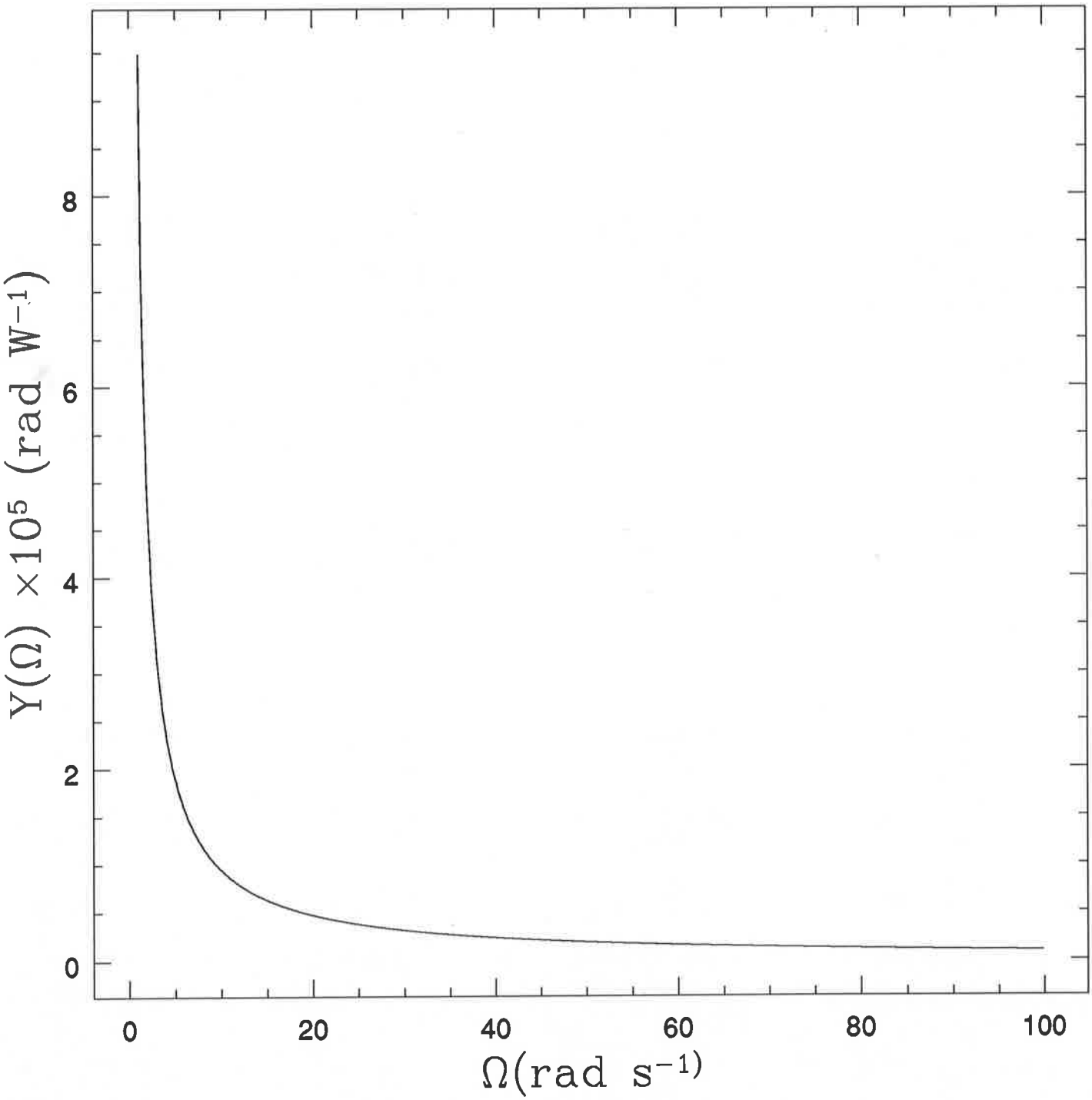

Fig 5

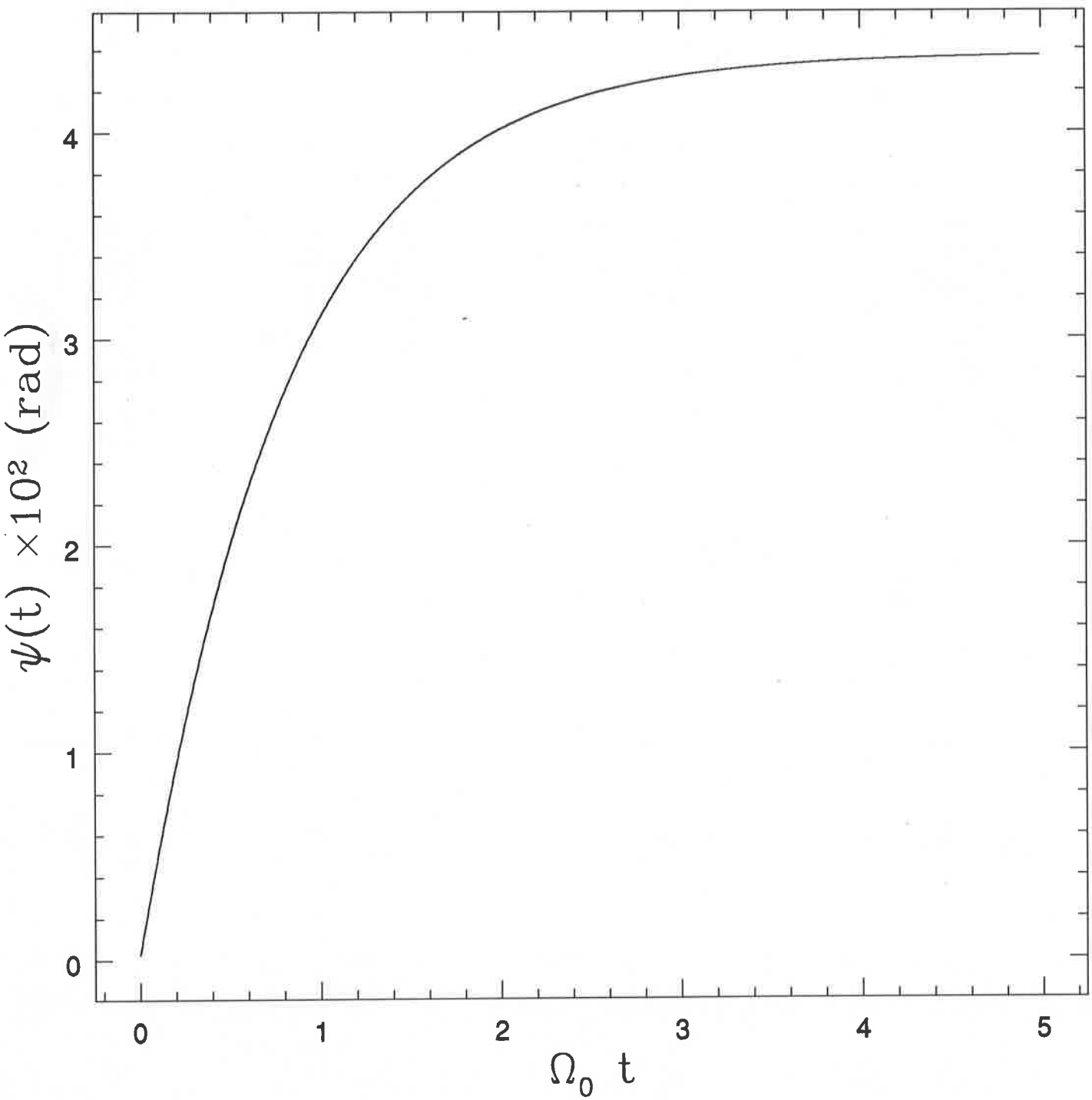

Fig 6